Application of Finite Control Set Model Based Predictive Method for Power Flow Control Using Unified Power Flow Controller

Amir Farakhor[1], Alireza E. Khosroshahi[1], Mehdi Abapour[1], Saeed Azimi Saadat[1]

[1]University of Tabriz, Tabriz, Iran
Amir_farakhor@yahoo.com, a.e.khosroshahi@gmail.com, abapour@tabrizu.ac.ir, s.azimi@tabrizu.ac.ir

Abstract

Unified Power Flow Controller (UPFC) is one of the most flexible, versatile and complex FACTS devices which are employed in the transmission systems to control the power flowing through the transmission line. In this paper, the application of the Finite Control Set Model Predictive Controller (FCS-MPC) is investigated for the power flow control using UPFC. FCS-MPC controller has several advantages such as simplicity, fast dynamic response and efficient computational realization. The presented controller predicts the future behavior of the controlled variables and by minimizing a cost function the best control actions can be taken. The prediction of the controlled variables requires some elaboration time. Therefore, to compensate the delay of the digital control system, the prediction of the controlled variables is performed two steps forward. The cost function is also defined as the deviation of the controlled variables from their reference values. The performance of the presented control strategy is assessed on UPFC connected two bus system. Simulation results indicate the effectiveness of the presented control algorithm.

1. Introduction

Implementation of new equipment consisting high power electronics based technologies such as Flexible Alternating Current Transmission Systems (FACTS) and proper controller design become essential for improvement of operation and control of power systems. Recent development of power electronics introduces the use of flexible ac transmission system (FACTS) controllers in power systems [1]. FACTS controllers are able to change, in a fast and effective way, the network parameters in order to achieve better system performance.

Of all the FACTS devices, the unified power flow controller (UPFC) is the most versatile and capable of providing stability to the system subjected to transient disturbances due to its ability. The UPFC controls, simultaneously or selectively, all parameters which effect on power flow in the transmission line, i.e. voltage amplitude and phase angle and series impedance of transmission line [2-8]. Because of its attractive features, modeling and controlling an UPFC have come into intensive investigation in the recent years. Several references in technical literature can be found on development of UPFC steady state, dynamic and linearized models. Steady state model referred as an injection model is described in [9]. Furthermore, the UPFC has been applied in a vast variety of control system investigations, which include neural network-based controller [10], fuzzy neural network approach [11], fuzzy control [12, 13], combination of fuzzy and PI controller [14], and controllers based on the optimization algorithms such as nonlinear optimal predictive controller [15] are some of the intelligent controllers presented in these papers. Recently, the use of nonlinear controllers in FACTS devices have been more attention.

Among the controllers which are used to control the FACTS devices, model predictive controller (MPC) has got a wide range of attractive and versatile features. Now a day, this controller is widely used in the field of industry as it has the ability to implement constraints in control process system.

In this paper, Finite Control Set Model Predictive Controller (FCS-MPC) has been chosen for the power flow control using UPFC. Attractive features of MPC method and UPFC jointly provide a very satisfactory solution to the power flow control. The performance of the presented control strategy is assessed on the UPFC connected two bus test system. The presented controller predicts the future behavior of the controlled variables and by minimizing a cost function the best control actions can be taken. The prediction of the controlled variables requires some elaboration time. Therefore, to compensate the delay of the digital control system, the prediction of the controlled variables is performed two steps forward. A studying example is carried out in MATLAB/Simulink and simulation results proves the power flow of the power systems is flexibly, real-timely and quickly controlled using the proposed controller.

2. Operation Principals of UPFC

The schematic of the Unified Power Flow Controller (UPFC) is shown in Fig. 1. UPFC comprises of two Voltage Source Converters (VSCs) which are connected via a common DC link. The series converter is connected in series with the transmission line using a Boosting Transformer (BT) and the shunt converter is in parallel with the transmission line through the Exciting Transformer (ET). The series converter injects an AC voltage with a controllable magnitude and phase angle in series with the transmission line. Therefore, the converter exchanges real and reactive power at its AC terminals through the series connected transformer. The shunt converter has two main objectives. First, the converter regulates the real power flow or DC link voltage control. The shunt converter provides the required real power at DC link. Therefore, the real power flows between the shunt and series converters through the common DC link. The other objective of the shunt converter is to exchange the reactive power so that the voltage of the shunt connected point could be regulated.

Fig. 2 shows the single line diagram of the test power system which the UPFC is installed. The UPFC is between the buses V_s and V_r and the shunt converter is connected to the bus 'V_s'. The current equations of the system can be expressed as follows:

$$\begin{bmatrix} \frac{di_{sea}}{dt} \\ \frac{di_{seb}}{dt} \\ \frac{di_{sec}}{dt} \end{bmatrix} = \begin{bmatrix} -\frac{R_{se}}{L_{se}} & 0 & 0 \\ 0 & -\frac{R_{se}}{L_{se}} & 0 \\ 0 & 0 & -\frac{R_{se}}{L_{se}} \end{bmatrix} \begin{bmatrix} i_{sea} \\ i_{seb} \\ i_{sec} \end{bmatrix} + \frac{1}{L_{se}} \begin{bmatrix} V_{sa} - V_{ra} - V_{sea} \\ V_{sb} - V_{rb} - V_{seb} \\ V_{sc} - V_{rc} - V_{sec} \end{bmatrix} \quad (1)$$

$$\begin{bmatrix} \frac{di_{sha}}{dt} \\ \frac{di_{shb}}{dt} \\ \frac{di_{shc}}{dt} \end{bmatrix} = \begin{bmatrix} -\frac{R_{sh}}{L_{sh}} & 0 & 0 \\ 0 & -\frac{R_{sh}}{L_{sh}} & 0 \\ 0 & 0 & -\frac{R_{sh}}{L_{sh}} \end{bmatrix} \begin{bmatrix} i_{sha} \\ i_{shb} \\ i_{shc} \end{bmatrix} + \frac{1}{L_{sh}} \begin{bmatrix} V_{sa} - V_{sha} \\ V_{sb} - V_{shb} \\ V_{sc} - V_{shc} \end{bmatrix} \quad (2)$$

Where R_{se}, L_{se}, and i_{se} are the resistance, inductance and the current of the transmission line and R_{sh}, L_{sh}, and i_{sh} are the resistance, inductance and the current of the shunt converter respectively. V_{se} and V_{sh} are the injected series and shunt voltages and V_s and V_r are the sending and receiving ends, respectively.

To obtain the DC link dynamic equation, the power losses of the converters can be neglected. The DC link dynamic equation can be expressed as:

$$P_{dc} = P_{se} + P_{sh} \quad (3)$$

$$i_{dc} = -C\frac{dV_{dc}}{dt} \quad (4)$$

The active power of the DC link is given as:

$$P_{dc} = V_{dc} i_{dc} = -CV_{dc}\frac{dV_{dc}}{dt} = -\frac{1}{2}C\frac{dV^2_{dc}}{dt} \quad (5)$$

$$\frac{dV^2_{dc}}{dt} = -\frac{2}{C}(P_{se} + P_{sh}) \quad (6)$$

Where C, V_{dc} and i_{dc} are the capacitance, voltage and current of the DC link, respectively.

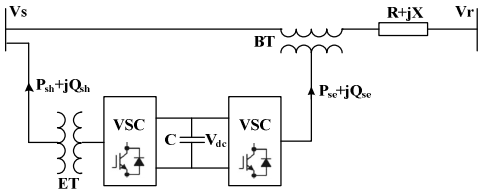

Fig.1: Schematic diagram of the UPFC system

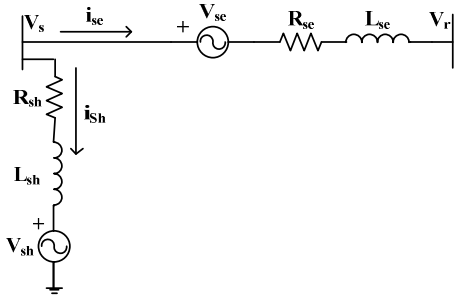

Fig.2: Schematic diagram of single phase representation of the power system with UPFC

3. Controller Design

The structure of the FACTS devices are based on PWM VSC modules. The control scheme applied in this paper for the power flow control using UPFC is Finite Control Set Model Predictive Control (FCS-MPC). Since the possible switching combination of the conventional two-level three-leg VSC is limited to eight, the FCS-MPC is an efficient and straightforward method to control the VSCs. The possible switching vectors for a two-level three-leg VSC are as follows:

$$\underline{S}(k) \triangleq \left\{ \begin{bmatrix} 0 \\ 0 \\ 0 \end{bmatrix}, \begin{bmatrix} 0 \\ 0 \\ 1 \end{bmatrix}, \begin{bmatrix} 0 \\ 1 \\ 0 \end{bmatrix}, \begin{bmatrix} 0 \\ 1 \\ 1 \end{bmatrix}, \begin{bmatrix} 1 \\ 0 \\ 0 \end{bmatrix}, \begin{bmatrix} 1 \\ 0 \\ 1 \end{bmatrix}, \begin{bmatrix} 1 \\ 1 \\ 0 \end{bmatrix}, \begin{bmatrix} 1 \\ 1 \\ 1 \end{bmatrix} \right\} \quad (7)$$

The controller determines the best switching vector at the time instant K so that a predefined cost function is minimized at the time instant $K+1$. The controlled variables must be estimated for the future time instants. Therefore, it is possible to determine the best switching vector among all possible switching vectors by minimizing a cost function. The cost function assures the tracking of the controlled variables from their reference values. However, the prediction of the controlled variables might be time consuming in comparison to the sampling time. Therefore, the delay compensation might be required.

3.1 Prediction of the Controlled Variables

The model predictive controller aims to estimate the future behavior of the controlled variables so that proper control actions could be determined. There are two VSCs in the structure of UPFC which are called the series and shunt converter. As it is mentioned before, the main objectives of the series converter are the real and the reactive power control. Therefore these controlled variables must be estimated for the future time instants.

The presented control strategy can be digitally implemented in the microprocessor based hardware. Therefore, the analysis must be developed in discrete mathematics in order to consider the delays, sampling time, and approximation. The Euler approximation is then used to obtain the discrete model of the system. The discrete model of the equation (1) can be expressed as follows:

$$\frac{di_{se}}{dt} = \frac{i_{se}(k) - i_{se}(k-1)}{T_s} \quad (8)$$

$$\begin{bmatrix} i_{sea}(k) \\ i_{seb}(k) \\ i_{sec}(k) \end{bmatrix} = \begin{bmatrix} \frac{L_{se}}{L_{se} + T_s R_{se}} & 0 & 0 \\ 0 & \frac{L_{se}}{L_{se} + T_s R_{se}} & 0 \\ 0 & 0 & \frac{L_{se}}{L_{se} + T_s R_{se}} \end{bmatrix} \begin{bmatrix} i_{sea}(k-1) \\ i_{seb}(k-1) \\ i_{sec}(k-1) \end{bmatrix} - \frac{1}{\frac{L_{se}}{T_s} + R_{se}} \begin{bmatrix} V_{sea}(K) \\ V_{seb}(k) \\ V_{sec}(K) \end{bmatrix} + \frac{1}{\frac{L_{se}}{T_s} + R_{se}} \begin{bmatrix} V_{sa}(k) - V_{ra}(k) \\ V_{sb}(k) - V_{rb}(k) \\ V_{sc}(k) - V_{rc}(k) \end{bmatrix} \quad (9)$$

By shifting (9) one step forward we have:

$$\begin{bmatrix} i_{sea}(k+1) \\ i_{seb}(k+1) \\ i_{sec}(k+1) \end{bmatrix} = \begin{bmatrix} \frac{L_{se}}{L_{se}+T_sR_{se}} & 0 & 0 \\ 0 & \frac{L_{se}}{L_{se}+T_sR_{se}} & 0 \\ 0 & 0 & \frac{L_{se}}{L_{se}+T_sR_{se}} \end{bmatrix} \begin{bmatrix} i_{sea}(k) \\ i_{seb}(k) \\ i_{sec}(k) \end{bmatrix} - \frac{1}{\frac{L_{se}}{T_s}+R_{se}} \begin{bmatrix} V_{sea}(k+1) \\ V_{seb}(k+1) \\ V_{sec}(k+1) \end{bmatrix} + \frac{1}{\frac{L_{se}}{T_s}+R_{se}} \begin{bmatrix} V_{sa}(k+1)-V_{ra}(k+1) \\ V_{sb}(k+1)-V_{rb}(k+1) \\ V_{sc}(k+1)-V_{rc}(k+1) \end{bmatrix} \quad (10)$$

Where, T_s is the sampling time. The injected series voltage with respect to the different switching combination can be expressed as follows:

$$\begin{aligned} V_{sea} &= \frac{V_{dc}}{3}(2S_a - S_b - S_c) \\ V_{seb} &= \frac{V_{dc}}{3}(2S_c - S_a - S_b) \\ V_{sec} &= \frac{V_{dc}}{3}(2S_b - S_c - S_a) \end{aligned} \quad (11)$$

Where S_a, S_b and S_c are equal to 1 if the corresponding device is on, 0 if the device is off. It is also considered that the main voltages V_s and V_r are constant during a sampling time T_s (V_s *(k+1)* $=V_s$ *(k)* and V_r *(k+1)* $=V_r$ *(k)*). Therefore, the future behavior of the currents flowing through the transmission line can be predicted by (10). To predict the future behavior of the currents (i_s) for all switching states according to (10) at time instant *K+1*, it is required to know the V_s, V_r and i_s at time instant *K*. The instantaneous active and the reactive power flowing through the transmission line can also be predicted as follows:

$$P_{se}(k+1) = \begin{bmatrix} V_{sa} & V_{sb} & V_{sc} \end{bmatrix} \begin{bmatrix} i_{sea}(k+1) \\ i_{seb}(k+1) \\ i_{sec}(k+1) \end{bmatrix} \quad (12)$$

$$Q_{se}(k+1) = \frac{1}{\sqrt{3}} \begin{bmatrix} V_{sbc} & V_{sca} & V_{sab} \end{bmatrix} \begin{bmatrix} i_{sea}(k+1) \\ i_{seb}(k+1) \\ i_{sec}(k+1) \end{bmatrix} \quad (13)$$

The shunt converter provides the required real power at DC link. Therefore, the real power flows between the shunt and series converters through the common DC link. The other objective of the shunt converter is to exchange the reactive power so that the voltage of the shunt converter connected point could be regulated. The real and reactive power flowing from the shunt circuit can also be predicted. The discrete model of (1) can be expressed as follows:

$$\begin{bmatrix} i_{sha}(k) \\ i_{shb}(k) \\ i_{shc}(k) \end{bmatrix} = \begin{bmatrix} \frac{L_{sh}}{L_{sh}+T_sR_{sh}} & 0 & 0 \\ 0 & \frac{L_{sh}}{L_{sh}+T_sR_{sh}} & 0 \\ 0 & 0 & \frac{L_{sh}}{L_{sh}+T_sR_{sh}} \end{bmatrix} \begin{bmatrix} i_{sha}(k-1) \\ i_{shb}(k-1) \\ i_{shc}(k-1) \end{bmatrix} - \frac{1}{\frac{L_{sh}}{T_s}+R_{sh}} \begin{bmatrix} V_{sha}(K) \\ V_{shb}(k) \\ V_{shc}(K) \end{bmatrix} + \frac{1}{\frac{L_{sh}}{T_s}+R_{sh}} \begin{bmatrix} V_{sa}(k) \\ V_{sb}(k) \\ V_{sc}(k) \end{bmatrix} \quad (14)$$

By shifting the (14) one step forward we have:

$$\begin{bmatrix} i_{sha}(k+1) \\ i_{shb}(k+1) \\ i_{shc}(k+1) \end{bmatrix} = \begin{bmatrix} \frac{L_{sh}}{L_{sh}+T_sR_{sh}} & 0 & 0 \\ 0 & \frac{L_{sh}}{L_{sh}+T_sR_{sh}} & 0 \\ 0 & 0 & \frac{L_{sh}}{L_{sh}+T_sR_{sh}} \end{bmatrix} \begin{bmatrix} i_{sha}(k) \\ i_{shb}(k) \\ i_{shc}(k) \end{bmatrix} - \frac{1}{\frac{L_{sh}}{T_s}+R_{sh}} \begin{bmatrix} V_{sha}(k+1) \\ V_{shb}(k+1) \\ V_{shc}(k+1) \end{bmatrix} + \frac{1}{\frac{L_{sh}}{T_s}+R_{sh}} \begin{bmatrix} V_{sa}(k+1) \\ V_{sb}(k+1) \\ V_{sc}(k+1) \end{bmatrix} \quad (15)$$

Similarly, the real and reactive power flowing from the shunt circuit can be calculated as follows:

$$P_{sh}(k+1) = \begin{bmatrix} V_{sa} & V_{sb} & V_{sc} \end{bmatrix} \begin{bmatrix} i_{sha}(k+1) \\ i_{shb}(k+1) \\ i_{shc}(k+1) \end{bmatrix} \quad (16)$$

$$Q_{sh}(k+1) = \frac{1}{\sqrt{3}} \begin{bmatrix} V_{sbc} & V_{sca} & V_{sab} \end{bmatrix} \begin{bmatrix} i_{sha}(k+1) \\ i_{shb}(k+1) \\ i_{shc}(k+1) \end{bmatrix} \quad (17)$$

3.2 Cost Function Definition

The control algorithm based on FCS-MPC can be described as follows:

1. Measurements which are required for the predictions of series and shunt power
2. Application of the switching state (calculated in the previous interval)
3. Estimation of the power at time instant *K+1*.
4. Cost function calculation for all the possible switching states.
6. Determination of the best switching state which minimizes the cost function.

The cost function is defined as the absolute value of the deviation of the controlled variables from their reference values as below:

$$J = \left|P^*_{se}(k+1) - P_{se}(k+1)\right| + \left|Q^*_{se}(k+1) - Q_{se}(k+1)\right| + \left|P^*_{sh}(k+1) - P_{sh}(k+1)\right| + \left|Q^*_{sh}(k+1) - Q_{sh}(k+1)\right| \quad (18)$$

The overall control scheme is shown in Fig. 3. First the prediction of the controlled variables is performed with consideration of the delay compensation. The reference values are also estimated for the future time. Then, the cost function is calculated for all possible switching states. The best switching combination which minimizes the cost function is determined and applied. In order to control the DC link voltage, a PI controller is used as it is shown in Fig. 3.

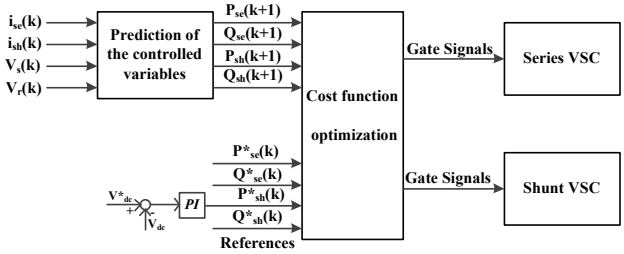

Fig.3: FCS-MPC block diagram of overall system

4. Simulation Results

To verify the performance of the presented control scheme, simulations have been carried out by Matlab/Simulink software on a two bus test system. The system parameters used in the simulation are as follows: the bus voltages are 220 kV and the initial phase of the sending bus is considered to be zero and the initial phase of the receiving end bus lags by 5 degrees. The base power is considered 100MVA. The boosting transformers turn ratio is considered 1:1 and the exciting transformers turn ratio is taken 1:10. The transmission line impedance is also 0.01+ j0.1 pu. The capacitance of DC link capacitor is also 500 µF.

The simulations are performed in two cases. First the dynamic performance of the system is assessed under step reference changes. At time instant (*t=1* sec) the reference value of the transmission line real power is changed from 40MW to 50MW and at time instant (*t=1.5* sec) it decreases to 35MW. Also, at time instant (*t=2* sec) the reference value of the transmission line reactive power is changed from -1MVAR to 0MVAR and at time instant (*t=2.5* sec) it decreases to -1.8MW. The real and reactive power of the system is shown in Fig. 4. As it is shown in Fig. 4, the series converter is well controlled so that the real and reactive powers flowing through the transmission line are tracked. In addition, at time instant (*t=3 sec*), the reference value of the reactive power flowing from the shunt circuit is altered from -2 MVAR to -2.5 MVAR and at time instant (*t=3.5* sec) it increases to -1.5MVAR. Also, at time instant (*t=4 sec*), the reference value of the DC link voltage is altered from 35kV to 45kV. Fig. 5 indicates the shunt circuit power flow and Fig. 6 depicts the DC link voltage. As it is shown in these figures, both the reactive power flowing from the shunt circuit and DC link voltage is controlled effectively. As it is shown in Fig. 5, the real power of the shunt circuit is surged at first and time instant (*t=4* sec) to charge the DC link then it regulates the real power flow between the series and shunt parts.

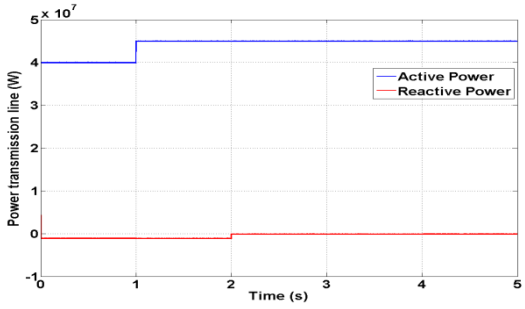

Fig.4: Transmission line power flow

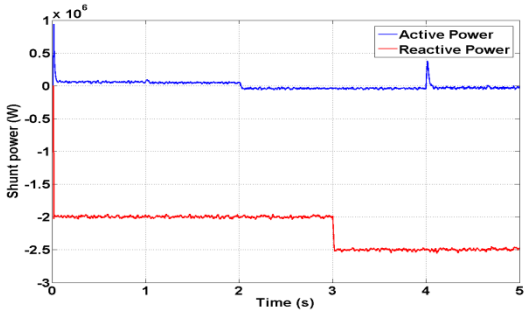

Fig.5: Shunt circuit power flow

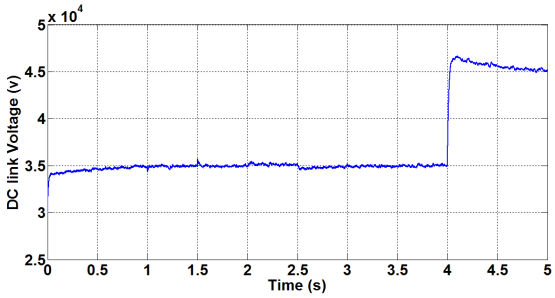

Fig.6: DC link voltage (reference step change at t=4s)

In second case, the performance of the system is evaluated under a sudden change of bus voltage phase. At time instant (*t=1 sec*), the phase of the receiving end bus is changed from -5 to -10 degrees. The real and reactive power flowing from the transmission line is fixed on 50MW and -1 MVAR respectively. The shunt reactive power is also -2 MVAR and the DC link voltage is 35 kV. Fig. 8 shows the power flow from the transmission line. Fig. 9 also shows the DC link voltage and the shunt reactive power. As it is shown in these figures, the system in not dramatically affected by sudden change of the receiving end bus phase and the system is efficiently controlled. Simulation results given in two cases validate the feasibility and flexibility of the presented control strategy under various conditions. The results also indicate a good dynamic response of the controller and zero steady state error.

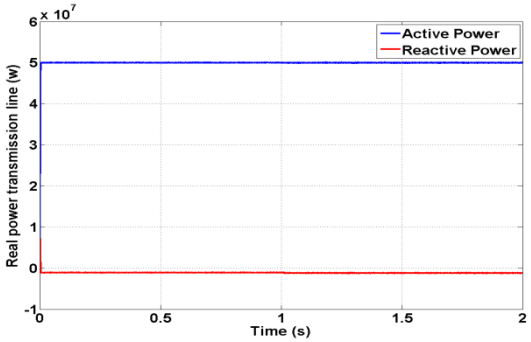

Fig.8: Transmission line power flow

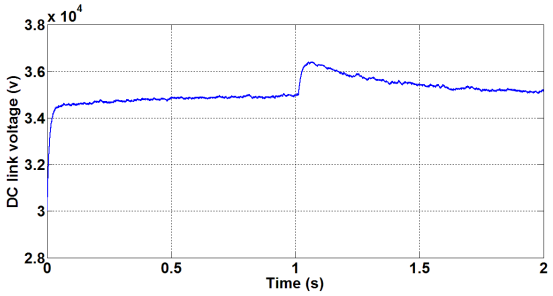

(a)

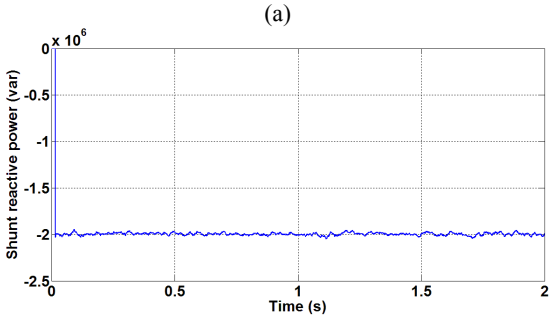

(b)

Fig.9: (a) DC link voltage, (b) Shunt circuit reactive power

5. Conclusion

In this paper, finite control set model predictive control scheme is applied on the UPFC. The presented control method along with the UPFC has the ability of the power flow control. The controlled parameters of the system are predicted for the future time instants. To improve the dynamic response of the system, calculation time delay is also compensated. Reference values are also estimated for future time instants using extrapolation. Simulation results confirm the feasibility of the control strategy in power flow control of the transmission line. The presented control scheme benefits from fast dynamic response and zero steady state error.

6. References

[1] R A. Laka, J.A. Barrena, M.A. Chivite-Zabalza, and J. Rodriguez, "Analysis and Improved Operation of a PEBB-Based Voltage-Source Converter for FACTS Applications," *IEEE Transaction. Power Delivery*, Vol. 28, No.3, pp. 1330 – 1338, 2013.

[2] L. Gyugyi, " Dynamic compensation of AC transmission lines by solid-state synchronous voltage sources," *IEEE Transaction. Power Delivery*, Vol. 9, No.2, pp. 904-911, 1994.

[3] Y. Shu-jun, S. Xiao-yan, W. Yan, Y. Yu-xin and Y. Zhi, "Research on dynamic characteristics of Unified Power Flow Controller (UPFC)," *Proceeding of 4th IEEE International Conference on Electric Utility Deregulation and Restructuring and Power (DRPT)*, pp. 490-493, 2011.

[4] L. Gyugyi, "Unified power-flow control concept for flexible AC transmission Systems," *IEE Proceedings Generation, Transmission and Distribution*, Vol. 139, No.4, pp. 323-331, 1992.

[5] K.M. Rogers and T.J. Overbye, "'Power flow control with Distributed Flexible AC Transmission System (D-FACTS) devices," *Proceeding of North American Power Symposium (NAPS)*, pp. 1-6, 2009.

[6] A. Nabavi-Niaki and M.R. Iravani, "Steady-state and dynamic models of unified power flow controller (UPFC) for power system studies," *IEEE Transaction. Power system*, Vol. 11, No.4, pp. 1934-1943, 1996.

[7] D.E. Soto-Sanchez and T.C. Green, "Voltage balance and control in a multi-level unified power flow controller," *IEEE Transaction. Power Delivery*, Vol. 16, No.4, pp. 732-738, 2001.

[8] A. Rajabi-Ghahnavieh, M. Shahidehpour, Fotuhi-Firuzabad and Feuillet, R., "UPFC for Enhancing Power System Reliability," *IEEE Transaction. Power Delivery*, Vol. 25, No.4, pp. 2881- 2890, 2010.

[9] M. Noroozian, L. Angquist, M. Ghandhari and G. Andersson., "Use of UPFC for optimal power flow control," *IEEE Transaction. Power Delivery,* Vol. 12, No.4, pp.1629-1634, 1997.

[10] S. Mishra, "Neural-network-based adaptive UPFC for improving transient stability performance of power system," *IEEE Transactions on Neural Networks*, Vol. 17, No.2, pp.461-470, 2006.

[11] T.T Ma, "P–Q decoupled control schemes using fuzzy neural networks for the unified power flow controller," *International Journal of Electronics and Power Energy System*,Vol. 29, pp. 748–758,2007.

[12] N.K. Sharma, P.P. Jagtap, "Modelling and application of unified power flow controller (UPFC)," *Proceeding of 3th International Conference on Emerging Trends in Engineering and Technology (ICETET)*, pp. 350–355, 2010.

[13] H. Na, L. Ruiye, X. Dianguo, "The Study of UPFC Fuzzy Control with Self-adjustable Factor," *Proceeding of Transmission and Distribution Conference and Exhibition: Asia and Pacific*, pp.1-5,2005.

[14] T.T., Ma, K.L. Lo, "Nonlinear power system damping control strategies for the unified power flow controller (UPFC)," *Proceeding of International Power Conference. Power System Technology,* pp. 673-678, 2000.

[15] H. Shayeghi, H.A. Shayanfar, S. Jalilzade and A. Safari, "COA based robust output feedback UPFC controller design," *Proceeding of* Energy Conversion Management.pp. 2678–2684, 2010.